Liquid freshwater transport and Polar Surface Water characteristics in the East Greenland Current during the AO-02 Oden expedition

Johan Nilsson [1]

Department of Meteorology, Stockholm University, SE-10691 Stockholm, Sweden

Göran Björk

Department of Oceanography, Earth Sciences Centre, Göteborg University, Box 460, SE-40530 Göteborg, Sweden

Bert Rudels

Finnish Institute of Marine Research, Box 2, FI-00561 Helsinki, Finland

Peter Winsor

Woods Hole Oceanographic Institution, Woods Hole, MA 02543, USA

Daniel Torres

Woods Hole Oceanographic Institution, Woods Hole, MA 02543, USA

Abstract

Dynamical features of the East Greenland Current (EGC) are synthesized from a survey conducted by the Swedish icebreaker *Oden* during the International Arctic Ocean - 02 expedition (AO-02) in May 2002 with emphasis on the liquid freshwater transport and Polar Surface Water. The data include hydrography and lowered Acoustic Doppler Current Profiler (LADCP) velocities in eight transects along the EGC, from the Fram Strait in the north to the Denmark Strait in the south. The survey reveals a strong confinement of the low-salinity polar water in the EGC to the continental slope/shelf—a feature of relevance for the stability of the thermohaline circulation in the Arctic Mediterranean. The southward transport of liquid freshwater in the EGC was found to vary considerably between the sections, ranging between 0.01 and 0.1 Sverdrup. Computations based on geostrophic as well as LADCP velocities give a section-averaged southward freshwater transport of 0.06 Sverdrup in the EGC during May 2002. Furthermore, *Oden* data suggest that the liquid freshwater transport was as large north of the Fram Strait as it was south of the Denmark Strait.

Preprint submitted to Elsevier Science *January 9, 2008*

Key words: East Greenland Current, late-winter observations, freshwater transport, Polar Surface Water

1 Introduction

Some 5 to 8 Sverdrup (Sv; 1 Sv = $1 \cdot 10^6$ m^3 s^{-1}) of warm Atlantic water enter the Arctic Mediterranean over the Greenland–Scotland Ridge (Hansen and Østerhus, 2000). As the Atlantic water circulates through the Arctic Mediterranean, it loses heat to the atmosphere and becomes less saline due to freshwater input. The action of these two transformation processes separates the Atlantic water into two circulation loops (cf. Rudels, 1995; Mauritzen, 1996). The major deep loop is determined mainly by the cooling occurring in the Norwegian Sea and the Barents Sea, which increases the density of the Atlantic water. This loop creates the dense deep waters of the Arctic Mediterranean and supplies the overflow water to the North Atlantic. The second weaker surface loop is dominated by the river runoff to and the melting of sea ice in the Arctic Ocean, forming the low salinity, less dense polar surface water. After following several and different circulation paths in the Arctic Mediterranean the waters of the two loops join the East Greenland Current in and north of Fram Strait. The less dense surface loop, augmented with Pacific Water from the Bering Strait (Jones et al., 1998), forms a low-salinity wedge near the coast above the denser water masses of the deep loop. The interaction between the two loops is limited but not absent. Ice formation in lee polynyas on the Arctic Ocean shelves may, through brine rejection, create waters saline and dense enough to supply the deeper loop, and the open ocean convection in the Greenland and Iceland Sea can bring low-salinity surface water, detached from the East Greenland Current, into the deep.

The Arctic Mediterranean receives a freshwater input of about 0.28 Sv, which originates from river runoff (0.13 Sv), net precipitation (0.06 Sv), and inflow of low-salinity Pacific water through the Bering Strait (0.09 Sv) (see Aagaard and Carmack, 1989; Dickson et al., 2007, and references therein) The freshwater supplied to the Arctic Mediterranean is exported to the North Atlantic west and east of Greenland, through the Canadian Arctic Archipelago and across the Greenland–Scotland Ridge, respectively. The freshwater transport east of Greenland is about 0.19 Sv of which 0.05 Sv is carried by the dense overflow waters (Dickson et al., 2007).

The freshwater in the EGC—should it enter the central Greenland Sea—has

[1] Corresponding author: email nilsson@misu.su.se; phone +46 8161736

the potential to decrease the surface density and thus reduce the convective activity and the associated deep-water production, hereby curtailing or disrupting the thermohaline exchange over the Greenland–Scotland Ridge (Stigebrandt, 1985). Thus, the transport and horizontal mixing of freshwater in the EGC are important for the operation and stability of the thermohaline circulation in the Arctic Mediterranean and the Nordic Seas (Aagaard and Carmack, 1989; Strass et al., 1993; Marotzke, 2000; Rahmstorf, 2000; Curry and Mauritzen, 2005).

It should be underlined that the freshwater budget of the Arctic Mediterranean remains relatively poorly known. To some extent, this reflects the difficulty to monitor the freshwater transport in the EGC, where severe ice conditions makes it difficult to conduct direct measurements. Thus, a key aim of the present work is to investigate the freshwater transport in the EGC on the basis of hydrographic and LADCP data collected during the Swedish Arctic Ocean Expedition 2002 (AO-02); see Rudels et al. (2005) for an overview of the physical oceanography of the AO-02. The measurements in the EGC were taken onboard the icebreaker *Oden* in May 2002. During the first half of May 2002, cold and clear weather conditions prevailed: despite the presence of the midnight sun, daily-mean air temperatures were below -10 °C and new ice was forming over the open leads. During the latter part of May, the temperatures were less harsh but the ice conditions remained severe in the EGC even south of the Denmark Strait. Thus, the present data set provides a unique picture of the late-winter conditions in the EGC all the way from north of the Fram Strait to south of the Denmark Strait; see Fig. 1.

2 Data and methods

The CTD system used during the AO-02 expedition was a Sea Bird 911+ instrument mounted on a 24-bottle rosette. For calibration purpose, salinities were measured onboard with a Guidline 8400B Autosal. Currents were measured by an Acoustic Doppler Current Profiler (LADCP), which was attached to the rosette sampler and equipped with dual (upward and downward looking) 300-kHz RDI Workhorse ADCPs.

The raw LADCP data were processed using an inverse technique described in Visbeck (2002) and detided by subtracting the barotropic tidal velocitiy as computed by a high-resolution (5 km) barotropic inverse tidal model (Padman and Erofeeva, 2004). The errors associated with the tidal model are primarily related to the errors of the input bathymetry. In the two northernmost sections the relative difference between the tidal-model bathymetry and measured depth was as high as 70 % at a few stations; in the more southerly sections the relative differences did not exceed 25 % and were generally on the order of

10 %. We estimate that relative error of the tidal-model velocities are roughly proportional to the relative error of the tidal-model bathymetry. The maximum tidal amplitudes in the sections range between 4 and 8 cm s^{-1}, except for in 70°N section where the tidal amplitude reaches 15 cm s^{-1}. Except for in the two northernmost sections (where the errors are larger), we estimate the tidal-model errors to be less than 3 cm s^{-1} on the shelf, decreasing to 1–2 cm s^{-1} offshore of the shelfbreak.

To analyze the freshwater transport, it is instructive to compute how the volume transport in the EGC are distributed between different salinities. For this purpose, we define a cumulative volume transport function with respect to salinity (Walin, 1977, 1982)

$$M(S) = -\int\int v(x,y,z)\, H[S - S_0(x,y,z)]\, dxdz, \tag{1}$$

where $v(x,y,z)$ is the velocity component normal to the section (counted positive when directed towards the Arctic), $S_0(x,y,z)$ the measured salinity, and H a unit step function; the integral covers a given section. As defined here, $M(S)$ gives the net southward transport of waters having salinities less than S in a chosen section of the EGC. Further, we define a cumulative area function $A(S)$ according to

$$A(S) = \int\int H[S - S_0(x,y,z)]\, dxdz, \tag{2}$$

which represents the area occupied, on a given section, by water having a salinity less than S. We also introduce a mean-velocity measure defined as

$$\overline{v}(S) = M(S)/A(S), \tag{3}$$

which is the mean velocity of the water having a salinity less than S.

To compute the freshwater transport in the EGC, we define a fractional freshwater content according to

$$\gamma(S) = \frac{(S_R - S)}{S_R}, \tag{4}$$

where S_R is a reference salinity taken to be 35.0. The freshwater transport, relative to the reference salinity S_R, is given by

$$M_F(S) = \int_0^S \frac{dM(S')}{dS'} \gamma(S')\, dS'. \tag{5}$$

Thus, $M_F(S)$ represents the southward volume flux of freshwater carried in the part of the section where the salinity is less than S. Analogously, the freshwater area, relative to the reference salinity S_R, is given by

$$A_F(S) = \int_0^S \frac{dA(S')}{dS'} \gamma(S')\, dS'. \tag{6}$$

When computing the transport functions $M(S)$ for the sections taken during AO-02, we will use two different velocity fields: the velocities obtained from the LADCP and the geostrophic velocities computed from the observed hydrography. In the latter case, the thermal wind relation is used, which states that

$$\frac{\partial v}{\partial z} = -\frac{g}{f\rho_0}\frac{\partial \rho}{\partial x}. \tag{7}$$

Here g is the acceleration of gravity, f the Coriolis parameter, and ρ_0 a constant reference density. To determine the absolute velocity from this formula, information on the velocity at some point in the water column is required. Although there tend to be southward near-bottom flows on the Greenland Slope (e.g. Foldvik et al., 1988; Woodgate et al., 1999; Fahrbach et al., 2001; Nøst and Isachsen, 2003; Schlichtholz, 2007), we set the bottom velocity to zero in the thermal wind calculation. This allows us to assess how the generally non-zero bottom velocities of the de-tided LADCP data affect the transport estimates. We will return to this issue when discussing the accuracy of the present transport computations.

In the evaluation of Eq. (1), we replace the integrals with sums. For each pair of stations, we compute the mean salinity and the geostrophic velocity down to the deepest common level with a vertical resolution of 1 m; hereafter we sum the transport contributions from each depth interval. By repeating the procedure for all pairs of stations in a given section, we obtain an estimate of $M(S)$. The method for estimating $A(S)$ is analogous.

Due to severe ice conditions, the AO-02 sections could not be extended all the way to the east coast of Greenland. The distance between the westernmost station and the coast in the sections ranged from 10 to 140 km; see Table 1. Thus, the transports and the area functions presented here miss some of the low salinity near-coastal waters in the EGC. This issue will be discussed further below.

3 Results

3.1 Hydrographic characteristics

The present focus is on the flow and the transformation of Polar Surface Water (PSW) along the EGC. This water mass of Arctic origin, which includes the Polar Mixed Layer and the halocline in the Arctic Ocean, is defined as having a potential temperature below zero degrees and a potential density lower than 27.7 kg m^{-3} (cf. Rudels et al., 1996, 2005). It is relevant to note that in the hydrographic sections presently considered, all water that have a salinity less than 34.5 belong to the PSW water mass. The PSW forms a near surface layer adjacent to the Greenland coast, and the hydrographic survey conducted by *Oden* reveals that the PSW is modified as it is carried southward in the East Greenland Current. The figures 2–7 show six transects in the EGC, ranging from the northernmost at 81°N to the southernmost at 66°N. An inspection of these transects reveals that the salinity of the PSW tends to increase southward. At 81°N, the near-coastal surface salinity is below 32, whereas it is about 33 in the section taken at 66°N. In addition, the vertical extent of the PSW (as measured by the depth of the -1°C–isotherm or 34–isohaline) increases slightly downstream. The 34 isohaline is encountered at a depth of about 100 m near the coast in the 81°N section. In the 66°N section, this isohaline reaches down to a depth of 170 m. Further, the bulk of the PSW tends to shift towards the continental shelf as one progresses southward. In the two northernmost sections, the 34 isohaline outcrops well seaward of the shelf break. In the more southerly sections, however, the 34 isohaline outcrops near the shelf break over isobaths in the range 300–500 m.

The two northernmost sections were completely ice covered. In the other sections, the ice edge was encountered in the surface salinity range 33.5 to 34.7; see Figs. 4–7. There was a tendency to find the ice edge at a lower salinity downstream in the EGC. It can further be noted that in the 75°N and 66°N sections, the ice edges were located in surface water with temperatures above the freezing point.

Along the section taken at 75°N, traversing the central Greenland Sea, the low-salinity core of the PSW was not encountered. In fact, the minimum salinity measured in this section ($S = 33.4$) was higher than that encountered in any of the other sections, including the section taken south of the Denmark Strait. Severe ice conditions at 75°N prevented *Oden* from surveying the innermost 50 km of the Greenland Shelf (see Fig. 1). Thus, it is possible that the low-salinity core of PSW was present in the near-shore region also at 75°N. This view is corroborated by the fact that the LADCP recorded shoreward velocities on the order of 10 cm s^{-1} on the westernmost part of the 75°N section. Further,

northerly winds prevailed when the section was occupied, implying that the surface Ekman layer transported water towards the Greenland Coast.

Figure 8 illustrates how the potential temperature–salinity characteristics measured at the near-coastal stations were modified along the East Greenland Current. The surface water, which is essentially at the freezing temperature, becomes more saline as one progresses downstream. The changes of the T–S characteristics of the PSW between 81°N and 72°N are likely caused by some combination of sea-ice formation and mixing within the body of PSW, rather than by mixing with the warmer and more saline Atlantic water masses (cf. Rudels et al., 2005). The fact that the potential temperature of the PSW remains close to the freezing point supports this interpretation. It should be noted that at 66°N, PSW was encountered only at the two innermost stations, which were taken some 50 km from the coast. Thus, along this section the core of the PSW was not sampled.

The area occupied by the PSW on the different sections is also a quantity of interest, which is listed in Table 1. We note that the 34-isohaline outcrops towards the east in all the sections, implying that $A(34)$ represents, for each section, the total area of the PSW between the eastward edge of the EGC and the westernmost hydrographic station. Analogously, $A_F(34)$ represents the total freshwater area (relative to $S_R = 35$) of the PSW in the sections. The area of the PSW varies between the sections, being roughly equivalent to that of a 100-m deep layer extending laterally some 50 to 100 km. It is interesting to note that the freshwater area $A_F(34)$ of the sections taken at 81°N, 72°N, and 70°N is nearly identical, corresponding to a one meter deep layer distributed over 50 km. In the Fram Strait at 79°N, $A(34)$ and $A_F(34)$ are significanly larger than in the other sections. Given that the westernmost station at 79°N was taken as far as 140 km from the Greenland Coast, it is evident that the real freshwater area in this part of the EGC was even greater. Assuming a mean-depth of 100 m and a salinity lower than 34 over the inner shelf would add $14 \cdot 10^6$ m^2 to $A(34)$ at 79°N, corresponding roughly to an increase of 50 %. In any event, the *Oden* data indicate the presence of a large pool of PSW in the western Fram Strait; a feature that is also seen in the hydrographic data presented by Bourke et al. (1987) and Schlichtholz and Houssais (1999). Also in the sections taken at 75°N and 66°N the near-coastal data gaps imply that significant contributions to $A(34)$ were missed; a 100 m deep layer of near-shore water with a salinity lower than 34 would roughly double the values of $A(34)$ in these two section. The near-coastal gaps in the hydrographic sections tend to change the true value of the freshwater area $A_F(34)$ in a similar fashion.

3.2 Velocity characteristics

The horizontal density gradients within the Polar Surface Water were relatively constant between the sections taken during AO-02. As illustrated in Figs. 2–7, the along-section density gradients generally give rise to southerly geostrophic velocities at the surface, which typically are on the order of 5–15 cm s^{-1} relative to the bottom. The mean geostrophic velocities of the PSW, defined as $\overline{v}(34) = M(34)/A(34)$, are given in Table 1. Further, the geostrophic velocities tend to peak in a surface-intensified jet, encountered over the continental slope in 500–900 m depth range. Most hydrographic sections also show the presence of somewhat weaker jets seaward as well as shoreward of the main jet. It can be noted that the horizontal density gradients were somewhat more pronounced at 70°N. Particularly strong northerly winds (on the order of 10–15 m s^{-1}) had been blowing for a few days when this section was taken. Thus, the sharp horizontal hydrographic gradients observed in this section were presumably created by a strong shoreward Ekman transport.

To examine the usefulness of the LADCP data for transport estimates, we compare the velocity fields obtained from the LADCP and the geostrophic calculation based on the hydrography. Figure 9 shows the north–south LADCP velocities for two pairs of neighbouring stations taken on the slope in the 79°N and the 72°N sections, respectively. For the two pairs of stations, also the mean LADCP velocity and the geostrophic velocity are illustrated (to facilitate comparison the bottom velocity of the former field has been added to the latter one). For the station pair from the 72°N section, the shear of the mean LADCP field is in good agreement with the geostrophic shear. At 79°N on the other hand, the two estimates disagree on the sign of the shear in parts of the upper water column. To some extent, this is attributable to the presence of an anticyclonic eddy within the PSW, visible as an anomalously weakly-stratified region near the shelf break in Fig. 3. Thus in this part of the 79°N section, the hydrography was not adequately resolved, hereby distorting the geostrophic shear estimate. An analysis of the AO-02 data reveals, however, that the LADCP shear tended to be in broad agreement with the thermal-wind shear over the shelf and the slope. In the deeper parts of the sections, where the horizontal density gradients were weak and the quality of the LADCP data tended to be poorer, the two shear estimates may deviate considerably.

The LADCP bottom velocities were generally southward over the Greenland Continental Slope, with the strongest flows encountered in the 79°N and 75°N sections. Here, southward bottom velocities on the order of 20 cm s^{-1} were measured over depths in the range 1500–2500 m. Results from moored current meters, reported by Woodgate et al. (1999) and Fahrbach et al. (2001), suggest that the long-term time-mean bottom velocities in these two sections are somewhat weaker, being on the order of 5–10 cm s^{-1}. On some stations

in the EGC the LADCP recorded northward bottom velocities on the slope, whereas moored current meters generally have shown southward mean bottom velocities over the entire slope. Thus, the instantaneous LADCP bottom velocities frequently include also time-dependent flow variations, which may reach strengths of 10 cm s^{-1} or more.

3.3 Volume transport estimates

We focus on the transport of Polar Surface Water in the East Greenland Current. From the above discussion, it is evident that neither the LADCP velocity nor the geostrophic flow provides reliable estimates of the time-mean velocity field. It is difficult, however, to assess which of the two velocity fields that yields the more accurate estimate of the time-mean transport. Therefore, we consider transport estimates based on the LADCP data as well as on the geostrophic flow relative to zero bottom velocity. (We have also calculated the transports using the geostrophic flow relative to the LADCP-derived bottom velocity. This procedure generally gives a transport that lies between the one obtained when the bottom velocity is set to zero and the LADCP-derived transport. These transports estimates are not further discussed here.)

Figure 10 illustrates the transport functions $M(S)$ for the two northernmost sections, calculated using the LADCP velocities as well as the geostrophic flow obtained from the thermal wind relation [i.e. Eq. (7)] assuming that the bottom velocity is zero. The two methods for computing $M(S)$ yield comparable transports at 81°N, whereas the two transport estimates differ in the 79°N section. We judge that the LADCP-derived velocities provide a better estimate of the instantaneous transports in the two sections. However, the LADCP-based estimate of $M(S)$ at 79°N, where an anticyclonic eddy was present, does presumably not represent the time-mean conditions that prevailed during the late-winter of 2002. Here, the instantaneous estimate of $M(S)$ gives a net northward transport of PSW in the salinity range between 33.3 and 34.2. This follows from the fact that

$$\frac{dM(S)}{dS}\,\Delta S, \tag{8}$$

gives the volume transport in the infinitesimal salinity interval between S and $S + \Delta S$. Thus, in a salinity interval where the derivative of M with respect to S is positive (negative) the net transport is directed towards (away from) the Atlantic. An analysis of the AO-02 data reveals that the net transport in this salinity range is directed towards the Atlantic in the other sections.

Figure 11 illustrates how the transport of PSW varied between the sections taken across the EGC during AO-02. The PSW transport is estimated by

$M(34)$ and $M(34.5)$ obtained from computations using LADCP-measured velocities as well as geostrophic velocities. Both velocity fields yield estimates of $M(34)$ and $M(34.5)$ that vary considerably between the sections. According to the geostrophic estimate of $M(34.5)$, the PSW transport in the AO-02 sections ranged from 0.5 to 2.0 Sv. Thus, the present estimates indicate that the transport of PSW generally varies along the EGC, implying zones where the PSW either converges or diverges. This is consistent with that fact the area of the PSW in the AO-02 sections varied, see Table 1.

Since the thermal-wind and LADCP-derived shears are generally in broad agreement, it is primarily the non-zero bottom velocity of the LADCP fields that cause the two estimates of $M(S)$ to differ. (A non-zero bottom velocity implies that a barotropic reference velocity has to be added to, or subtracted from, the geostrophic velocity profile.) Figure 11 shows that relative to the geostrophic case with zero bottom flow, the LADCP-estimated instantaneous bottom velocity may either enhance or reduce the transport of Polar Surface Water. The fact that the instantaneous bottom velocities do not modify the transports in a systematic way suggests that the bottom velocities measured from *Oden* include time-dependent barotropic motions, either forced by wind variations or associated with tidal currents (which would imply an inaccurate detiding procedure). The anomalously large LADCP-based estimate of $M(34.5)$ at 72°N was due to a strong bottom flow (on the order of 20 cm s^{-1}) on the slope, encountered at a depth of about 1500 m. This barotropic flow component enhanced the near-surface advection of the PSW in the salinity range between 34 and 34.5, which extended out over the slope (see Fig. 5). At 70°N, the reduction of the LADCP transports relative to the geostrophic ones were caused by an intense northward bottom flow at single station on the shelf: At the second station from the coast, where the 34.5 isohaline surface reached its maximum depth (see Fig. 6), a northward bottom velocity of almost 20 cm s^{-1} was recorded; elsewhere on the shelf southward bottom velocities on the order of 10 cm s^{-1} were found.

In the Fram Strait at 79°N, the present estimates of $M(34.5)$ suggest a southward transport of PSW ranging from 1.3 to 1.9 Sv. This is in broad agreement with other existing estimates of the transport of PSW in the Fram Strait. Using a one-year record of moored current data, Foldvik et al. (1988) obtained a PSW transport of 1 Sv. Based on an analysis of hydrographic data collected in the summer of 1984, Schlichtholz and Houssais (1999) estimated that the southward transport of PSW was 1.1 Sv. It should be noted that the flow of PSW constitutes only a small part of the total transport in the EGC: In the Fram Strait, the total southward volume transport is on the order of 10 Sv (e.g. Fahrbach et al., 2001). In the EGC at 75°N, Woodgate et al. (1999) estimated a total annual-mean southward transport on the order of 20 Sv. Based on the water-mass composition of the flow, they argued that less than 50 % of the total transport is associated with the long-range through flow, whereas

the remainder of the transport recirculates locally in the Greenland Sea Gyre.

A number of factors contribute to the uncertainty of the AO-02 transport calculations. First of all, there is the lack of data between the westernmost station of the sections the Greenland Coast. Even in the sections, there is a limited sampling of the hydrography. Moreover, there are errors in the LADCP velocities, arising from instrumental limitations and inaccuracies of the detidal procedure. One way to quantify how velocity errors affect the transport estimates is to add a uniform velocity anomaly (say δv) over the sections. The resulting transport anomaly is $\delta M(S) = \delta v \cdot A(S)$. Using the mean-velocity measure $\overline{v}(S) = M(S)/A(S)$, we can write $\delta M/M = \delta v/\overline{v}$. This shows that the relative transport error is proportional to the relative velocity error. To examine the influence of velocity errors, we compute the transport anomaly $\delta M(34) = \delta v \cdot A(34)$ caused by a uniform velocity anomaly (or error) of 0.05 m s^{-1}. The resulting transport anomalies are given in Table 2. Note that the constant velocity error δv gives a large transport error in the sections with large $A(34)$; the relative transport error is large in the sections with weak mean geostrophic velocity $\overline{v}(34)$. For instance, at 79°N a uniform velocity error of 0.05 m s^{-1} would give relative transport error of 100 %; whereas at 66°N the corresponding transport error would be about 40 %. We underline that the anomalies given in Table 2 should be viewed as upper bounds of the transport errors. The errors of the LADCP velocities should generally be less than 0.03 m s^{-1} and it is unlikely that the error should be uniform over an entire section.

3.4 Freshwater transport estimates

We proceed to estimate the liquid freshwater transport in the East Greenland Current, which is obtained by calculating the function $M_F(S)$; see Eq. (5). Here, $M_F(S)$ is calculated relative to the salinity 35, which characterizes the Atlantic water entering the Arctic Ocean. Further, we focus on the freshwater transport associated with the flow of Polar Surface Water in the EGC. A key aim is to examine how the PSW flux of liquid freshwater from the Arctic Ocean varied downstream in the EGC during the AO-02. The freshwater transports are summarized in Figs. 12, 13 and Table 2, which also gives the freshwater transport anomalies $\delta M_F(34)$ resulting from a uniform velocity anomaly (or error) of 0.05 m s^{-1}; see the discussion of the volume transport anomalies above. Note also that the 34.5 isohaline surface does not outcrop in the two northernmost sections (see Figs. 2 and 3), implying that the estimates of $M_F(34.5)$ there may miss some transport to the east of the sections.

Figure 12, showing the functions $M_F(S)$ calculated using geostrophic velocities, exhibits a few noteworthy features. To begin with, the derivative of

$M_F(S)$ with respect to S is positive in all sections for $S < 34.5$. Thus, the geostrophic AO-02 estimates yield a net southward freshwater flux within the entire body of PSW in the EGC, i.e. there was no northward freshwater transport in any salinity interval. This follows from the discussion in connection with Eq. (8). Further, the strongest flux per unit salinity (i.e. the largest derivative of $M_F(S)$) is found for the lowest salinity of a given section. This reflects, in addition to the obvious fact that low salinity water transports relatively more freshwater, the presence of the Polar Mixed Layer, which has an essentially uniform salinity and thus contributes with a significant transport in a narrow salinity interval. It can also been noted that the freshwater flux is shifted towards higher salinities as one moves southward in the EGC.

We proceed to consider the along-stream variations of the freshwater transport based on the geostrophic velocities. Figure 13 shows that, in a given section, $M_F(34)$ is consistently smaller than $M_F(34.5)$ and that these two transport measures covary along the EGC. The geostrophic estimates of $M_F(34)$ as well as of $M_F(34.5)$ are comparable at 81°N and 66°N. Thus, the AO-02 hydrographic data suggests that the freshwater transport carried by the PSW was as large north of the Fram Strait as it was south of the Denmark Strait. It should be emphasized that the PSW was encountered only on the two innermost stations at 66°N and that the westernmost station was taken some 40 km from the Greenland Coast. Accordingly, only a smaller fraction of the PSW was surveyed by *Oden* at 66°N, suggesting that the present data may underestimate the freshwater transport in this section. As expected, the estimated freshwater transport was small in the central Greenland Sea at 75°N, where hardly any low-salinity PSW was encountered. Excluding this anomalous section, our geostrophic estimates of $M_F(34.5)$ range between 0.04 and 0.08 Sv. The strongest geostrophic transports are encountered in the 79°N and 70°N sections, where the freshwater fluxes are nearly similar. At 79°N, it is the large area extent of the PSW that gives rise to the high transport; whereas at 70°N the high transport is primarily created by anomalously strong geostrophic velocities (see Figs. 3 and 6). It should be pointed out that the 79°N section was terminated near 10°W, some 140 km east of the Greenland Coast. The hydrographical study of Bourke et al. (1987) suggests the presence of a northward flow shoreward of 10°W, a feature related to an anticyclonic circulation pattern on the East Greenland Shelf. Thus, at 79°N we may overestimate the southward freshwater transport, as some northward transport could have occurred on the shelf west of 10°W.

Also the LADCP-derived freshwater transports exhibit a strong variability between the different AO-02 sections. Figure 13 illustrates that the non-zero bottom flow of the LADCP velocity field may increase as well as decrease the freshwater transport relative to the geostrophic calculation. In the 70°N and 66°N sections, for instance, bottom velocities towards the Arctic on the shelf reduced the LADCP-derived freshwater transports. This illustrates once more

that the LADCP bottom velocities to some extent include time-dependent barotropic flows. Thus, although the LADCP data should yield a better estimate of the instantaneous transports, the geostrophic calculation may provide a better estimate of the time-mean transports during May 2002. It should be noted, however, that the along-stream variations of the geostrophic transport as well as the freshwater area most likely also reflect time variations of the flow. In any event, the uncertainty regarding the time-mean bottom flow should be the main error source in the AO-02 freshwater transport calculations; see the transport anomalies $\delta M_F(34)$ listed in Table 2.

4 Discussion

The late-winter measurements taken during the AO-02 expedition indicate that the transport of low-salinity Polar Surface Water in the East Greenland Current may vary considerably along stream. The present estimates of the liquid freshwater transport in the EGC reflect this variability and accordingly provide a range of transports (see Table 2). The freshwater transport, represented by $M_F(34.5)$, varies in the AO-02 sections from 0.01 to 0.09 Sv. Disregarding the 75°N section, the geostrophic estimates suggest that the Polar Surface Water in the EGC carried at least 0.04 Sv of freshwater. This estimate was obtained by assuming zero flow at the bottom, and should thus serve as a lower bound on the freshwater transport. By excluding the 75°N section, the average of $M_F(34.5)$ for the sections in the EGC is 0.06 Sv, with a standard deviation of 0.02 Sv. For the LADCP-based estimates of $M_F(34.5)$, the corresponding average is also 0.06 Sv, with a standard deviation of 0.03 Sv. Based on these results, we judge that during the AO-02 the Polar Surface Water in East Greenland Current carried about 0.06 Sv of freshwater and that the bulk of it exited into the Atlantic through the Denmark Strait.

Since it was not possible to continue the sections all the way to the shore, the AO-02 survey may systematically have missed a significant part of the freshwater flux. However, we believe that the present data nevertheless captured the main freshwater transport, except in the sections taken at 75°N and 66°N where the low salinity PSW was poorly sampled. The main reason is that a baroclinic geostrophic flow requires a horizontal density gradient. Thus to sustain a baroclinic geostrophic flow, the unobserved zone near the coast must have contained even fresher water than measured at the innermost station in the section. This would require surface salinities well below 32, which even during summer are rarely observed in the Arctic Ocean north of Fram Strait (Björk et al., 2002). Accordingly, we consider it unlikely that there were strong baroclinic flows near the coast. Furthermore, the 70°N section, which was terminated rather close to the shore (10 km), did not reveal the presence of any exceptionally low salinity surface water. However, the pres-

ence of barotropic flows towards the Atlantic over the inner shelf could still have increased the near-shore freshwater transport. In fact, it is likely that the prevailing northerly winds along the East Greenland Shelf force a barotropic flow towards the Atlantic that essentially follows the isobaths. In a steady state, the bottom stress of the isobath-following barotropic flow balances the surface wind stress (see e.g. Walin, 1972; Nøst and Isachsen, 2003; Nilsson et al., 2005). For a mean wind speed of 5 m s^{-1}, such a frictionally-balanced barotropic flow could reach a strength of about 0.1 m s^{-1} (cf. Nøst and Isachsen, 2003). In the 66°N section, where the innermost 40 km of the shelf was not surveyed, we estimate that the presence of a near-shore barotropic flow of 0.1 m s^{-1} would more than double the freshwater transport. This would give a freshwater transport at 66°N which is comparable to the one estimated at 70°N, where the innermost station was taken 10 km from the coast.

The data collected during the AO-02 expedition reveal no immediate signs of a leakage of low-salinity water and ice from the EGC into the ice-free part of the Nordic Seas. To begin with, no low-salinity eddies or near-surface freshwater caps were observed east of the front/pack-ice edge. To some extent, the persistent northerly winds served to confine the freshwater and sea ice towards the coast, creating a sharp ice edge (observed from the ship and visible in satellite images). Further, the fact that the AO-02 freshwater transport estimates are comparable in northern- and southern-most sections suggests an approximate along-stream conservation of the liquid freshwater. Two effects are known to change the liquid freshwater transport along stream in the EGC: an eastward freshwater leakage of about 0.015 Sv occurring in the Jan Mayen Current and the East Icelandic Current (Dickson et al., 2007); and melting of sea ice, which causes the annual-mean liquid freshwater transport to increase downstream by 50% from the Fram Strait to the Denmark Strait (Aagaard and Carmack, 1989; Dickson et al., 2007). It should be noted that the eastward freshwater leakage in the Jan Mayen Current and the East Icelandic Current is smaller than the inter-section standard deviation of the AO-02 freshwater transports. Furthermore, freezing rather than melting of sea ice occurred in the EGC during the AO-02 expedition, implying some downstream decrease of the liquid freshwater transport. In summary, the late-winter AO-02 data suggest a negligible leakage of liquid freshwater from the EGC.

A situation without leakage of liquid freshwater from the EGC does not imply that the flow must be non-divergent along the coast. The AO-02 data reveal along-stream variations of the freshwater transport and the freshwater area in the EGC. Spatial variations of the onshore Ekman transport is one mechanism that may perturb the content and flow of Polar Surface Water along the EGC. Once created, such disturbances should move downstream (either advected by the mean flow or propagated as coastal waves). Using 0.1 m s^{-1} as a typical velocity of the EGC gives an advection time of about 8 months from 81°N to 66°N.

It is relevant to compare the present late winter-time estimate of the liquid freshwater transport in the EGC with other existing estimates; see table 3. Dickson et al. (2007) gives a compilation of freshwater transport estimates in the Arctic and Nordic Seas. For the Fram Strait, they suggest a mean equatorward freshwater transport of 0.15 Sv, which is comprised of ice export (0.09 Sv), upper water or PSW export (0.05 Sv), and exchange of intermediate and Atlantic waters (0.01 Sv). It is interesting to note that the present estimate obtained at 79°N in the Fram Strait is comparable to the late-summer estimates by Meredith et al. (2001) based on moored current meters. For the period from August to September they reported values ranging between 0.06 Sv (in 1998) and 0.12 Sv (in 1997). For May 2002, our geostrophic estimate of the freshwater flux in the Fram Strait is about 0.07 Sv. Thus, the AO-02 data indicate that the EGC transports roughly as much liquid freshwater in late winter as it does in late summer. This view is also supported by the Fram Strait results of Schlichtholz and Houssais (1999), who presented geostrophic estimates based on observed summer hydrography, and of Holfort and Hansen (2004), who presented estimates based on observed currents and summer hydrography; see table 3. Another relevant transport estimate is given by Oliver and Heywood (2003), who report the results based on a hydrographic survey, which traversed the entire Nordic Seas in the summer of 1999. Their analysis, which included direct current measurements, yielded an equatorward freshwater transport on the order of 0.10 Sv.

The main focus of the present work has been on the liquid freshwater transport associated with the flow of Polar Surface Water, characterized by salinities less than 34.5. As shown in Fig. 12 for the geostrophic calculations, the transport functions $M_F(S)$ generally tend to increase all the way to 35 (the reference salinity in the computation). This reflects the freshwater transport accomplished by more saline denser water masses, e.g. Return Atlantic Water and overflow waters (cf. Rudels et al., 2005). In the LADCP-based calculations, the contribution to the freshwater transport from the more saline water masses can be quite large: The values of $M_F(35)$ in the sections from 81°N to 70°N are 0.09, 0.13, 0.07, 0.20, and 0.05 Sv, respectively. For the LADCP-based calculation in the 72°N section, $M_F(35)$ is nearly twice as large as $M_F(34.5)$, suggesting a 0.1 Sv freshwater transport in the salinity range between 34.5 and 35. Given that the freshwater transport due to the Greenland–Scotland Ridge dense overflow is estimated to about 0.05 Sv (Dickson et al., 2007), it is likely that the present high LADCP-based freshwater transports in the salinity range between 34.5 and 35 reflect time-dependent flow or include a transport component that recirculate within the Nordic Seas.

In summary, the late-winter AO-02 data yield a liquid freshwater transport in the EGC on the order of 0.06 Sv. This transport falls within the range of previous estimates in the Fram Strait. However, it should be underlined that the present results show that the freshwater transport of the EGC varies

considerable in time as well as along stream, demonstrating that long-term observations or repeated measurement are required to obtain representative transport estimates.

Acknowledgements

We wish to thank the Captain and the Crew of IB *Oden* for their assistance and support during the cruise and the Swedish Polar Secretariat for logistic support. We also thank two anonymous reviewers for valuable comments. Financial support was provided by the Swedish Research Council (JN and GB), the Ivar Bendixson Foundation (JN), The European Commission programme ASOF-N (contract No EVK2-CT-2002-00139), ASOF-W (contract No EVK2-CT-2002-00149), DAMOCLES (contract No 0189509) (BR), the National Science Foundation (PW, through grant OPP-0352628) and a fellowship at the Woods Hole Oceanographic Institution's Ocean and Climate Change Institute (PW).

References

Aagaard, K. and E. C. Carmack, 1989: The role of sea ice and other fresh water in the Arctic circulation. *J. Geophys. Res.*, **94 (C10)**, 14485–14498.

Björk, G., J. Söderqvist, P. Winsor, A. Nikolopoulos and M. Steele, 2002: Return of the cold halocline to the Amundsen Basin of the Arctic Ocean: implications for the sea ice mass balance. *Geophys. Res. Lett.*, **29**, doi:10.1029/2001GL015147.

Bourke, R. H., J. L. Newton, R. G. Paquette and M. D. Tunnicliffe, 1987: Circulation and water masses of the East Greenland Shelf. *J. Geophys. Res.*, **92 (C7)**, 6729–6740.

Curry, R. and C. Mauritzen, 2005: Dilution of the northern North Atlantic in recent decades. *Science*, **308**, 1772–1774.

Dickson, B., B. Rudels, S. Dye, M. Karcher, J. Meincke and I. Yashayaev, 2007: Current estimates of the freshwater flux through Arctic and subarctic seas. *Progress In Oceanography*, **73**, 210–230.

Fahrbach, E., J. Meincke, S. Østerhus, G. Rohardt, U. Schauer, V. Tverberg and J. Verduin, 2001: Direct measurements of volume transports through Fram Strait. *Pol. Res.*, **20 (2)**, 217–224.

Foldvik, A., K. Aagaard and T. Tørresen, 1988: On the velocity field of the East Greenland Current. *Deep Sea Res.*, **35**, 1335–1354.

Hansen, B. and S. Østerhus, 2000: North Atlantic - Nordic Seas exchanges. *Progress In Oceanography*, **45**, 109–208.

Holfort, J. and E. Hansen, 2004: Report on the freshwater fluxes through the Fram Strait (preliminary results). Report to ASOF-N, 6 pp. with 8 figures.

Jones, E. P., L. G. Anderson and J. H. Swift, 1998: Distribution of Atlantic and Pacific Water in the upper Arctic Ocean: implications for the circulation. *Geophys. Res. Lett.*, **25 (6)**, 765–768.

Marotzke, J., 2000: Abrupt climate change and the thermohaline circulation: Mechanisms and predictability. *P. Natl. Acad. Sci. USA*, **97**, 1347–1350.

Mauritzen, C., 1996: Production of dense overflow waters feeding the North Atlantic across the Greenland-Scotland Ridge. Part 1: Evidence for a revised circulation scheme. *Deep-Sea Res.*, **43**, 769–806.

Meredith, M., K. Heywood, P. Dennis, L. Goldson, R. White, E. Farbach and S. Østerhus, 2001: Freshwater fluxes through the western Fram Strait. *Geophys. Res. Lett.*, **28**, 1615–1618.

Nilsson, J., G. Walin and G. Broström, 2005: Thermohaline circulation induced by bottom friction in sloping-boundary basins. *J. Mar. Res.*, **63**, 705–728.

Nøst, O. A. and P. E. Isachsen, 2003: The large-scale time-mean ocean circulation in the Nordic Seas and the Arctic Ocean estimated from simplified dynamics. *J. Mar. Res.*, **61**, 175–210.

Oliver, K. I. and K. J. Heywood, 2003: Heat and freshwater fluxes through the Nordic Seas. *J. Phys. Oceanogr.*, **33**, 1009–1026.

Padman, L. and R. Erofeeva, 2004: A barotropic inverse tidal model for the Arctic Ocean. *Geophys. Res. Lett.*, **31 (2)**, Art. No. L02303.

Rahmstorf, S., 2000: The thermohaline ocean circulation: a system with dangerous thresholds? *Climatic Change*, **46**, 247–256.

Rudels, B., 1995: The thermohaline circulation of the Artic Ocean and the Greenland Sea. *Phil. Trans. R. Soc. Lond.*, **352**, 287–299.

Rudels, B., L. G. Anderson and E. P. Jones, 1996: Formation and evolution of the surface mixed layer and the halocline of the Artic Ocean. *J. Geophys. Res.*, **101 (C4)**, 8807–8821.

Rudels, B., G. Björk, I. Lake, C. Nohr, J. Nilsson and P. Winsor, 2005: The interaction between waters from the Arctic Ocean and the Nordic Seas north of the Fram Strait and along the East Greenland Current: results from the AO-02 Oden expedition. *J. Mar. Systems*, **55**, 1–30.

Schlichtholz, P., 2007: Density-dependent variations of the along-isobath flow in the East Greenland Current from the Fram Strait to the Denmark Strait. *J. Geophys. Res.*, **112**, C12022, doi:10.1029/2006JC003987.

Schlichtholz, P. and M.-N. Houssais, 1999: An invers modeling study in the Fram Strait. Part II: water mass distribution and transports. *Deep-Sea Res.*, **II 46**, 1137–1168.

Stigebrandt, A., 1985: On the hydrographic and ice conditions in the northern North Atlantic during different phases of a glaciation cycle. *Palaeogeogr., Palaeoclimatol., Palaeoecol.*, **50**, 303–321.

Strass, V. H., E. Fahrbach, U. Schauer and L. Sellmann, 1993: Formation of Denmark Strait overflow water by mixing in the East Greenland Current.

J. Geophys. Res., **98**, 6907–6919.

Visbeck, M., 2002: Deep velocity profiling using lowered acoustic doppler current profilers: Bottom track and inverse solutions. *J. Atmos. Ocean Tech.*, **19**, 794–807.

Walin, G., 1972: On the hydrographic response to transient meteorological disturbances. *Tellus*, **24**, 169–186.

Walin, G., 1977: A theoretical framework for the description of estuaries. *Tellus*, **29**, 128–136.

Walin, G., 1982: On the relation between sea-surface heat flow and thermal circulation in the ocean. *Tellus*, **34**, 187–195.

Woodgate, R. A., E. Fahrbach and G. Rohardt, 1999: Structure and transport of the East Greenland Current at 75°N from moored current meters. *J. Geophys, Res.*, **104 (C8)**, 18059–18072.

Section	Days	Distance	$A(34)$	$A_F(34)$	$\overline{v}(34)$
81°N	06–10	40 km	$9 \cdot 10^6$ m^2	$53 \cdot 10^4$ m^2	0.07 m s^{-1}
79°N	12–14	140 km	$24 \cdot 10^6$ m^2	$118 \cdot 10^4$ m^2	0.05 m s^{-1}
75°N	16–18	50 km	$4 \cdot 10^6$ m^2	$15 \cdot 10^4$ m^2	0.03 m s^{-1}
72°N	19–21	20 km	$12 \cdot 10^6$ m^2	$54 \cdot 10^4$ m^2	0.06 m s^{-1}
70°N	26–27	10 km	$11 \cdot 10^6$ m^2	$52 \cdot 10^4$ m^2	0.12 m s^{-1}
66°N	29–30	40 km	$6 \cdot 10^6$ m^2	$27 \cdot 10^4$ m^2	0.13 m s^{-1}

Table 1
The observed area $A(34)$ of PSW having a salinity less than 34 and the associated freshwater area $A_F(34)$ (relative to a reference salinity of 35) of the AO-02 sections; see Eqs. (2) and (6) for definitions. The mean velocity of the PSW, counted positive for flow towards the Atlantic, is computed as $\overline{v}(34) = M(34)/A(34)$ using the geostrophic estimate of $M(34)$; see Eq. (2) and Table 2. Here "Days" refers to the dates in May 2002 during the sections were taken and "Distance" gives distance between westernmost station and the coast.

Section	$M(34)$ (Sv)	$\delta M(34)$ (Sv)	$M(34.5)$ (Sv)	$M_F(34)$ (mSv)	$\delta M_F(34)$ (mSv)	$M_F(34.5)$ (mSv)
81°N	0.6 (0.7)	0.4	1.2 (2.2)	35 (41)	26	47 (71)
79°N	1.2 (0.6)	1.2	1.9 (1.3)	60 (38)	59	75 (52)
75°N	0.1 (0.3)	0.2	0.6 (1.4)	4 (9)	8	13 (31)
72°N	0.7 (0.9)	0.6	1.5 (3.6)	34 (40)	27	50 (95)
70°N	1.3 (1.0)	0.6	2.1 (1.1)	62 (52)	26	78 (55)
66°N	0.8 (0.4)	0.3	0.9 (0.7)	34 (16)	14	37 (22)

Table 2
Estimates of volume and freshwater transports within the body of Polar Surface Water having a salinity less than 34 and 34.5, respectively. Positive values implies transports towards the Atlantic and the freshwater transport are given in units of milli-Sverdrup (mSv). Results based on thermal wind velocities relative to zero flow at the bottom and the LADCP data are included (the latter are given within parentheses). The freshwater transports are calculated for a reference salinity of 35; see Eq. (5). Also shown are the transport changes $\delta M(34) = \delta v \cdot A(34)$ and $\delta M_F(34) = \delta v \cdot A_F(34)$ caused by a constant velocity anomaly δv of 0.05 m s^{-1}.

Study	Period	S_R	Freshw. flux
Aagaard and Carmack (1989)	"Climatology"	34.8	26 / 820
Schlichtholz and Houssais (1999)	Summer 1984	34.93	63 / 2000
Meredith et al. (2001)	Aug.-Sept. 1997	34.92	117 / 3680
Meredith et al. (2001)	Aug.-Sept. 1998	34.92	63 / 2000
Holfort and Hansen (2004)	Sept. 2003	34.9	38 / 1230
Dickson et al. (2007)	"Climatology"	35.2	49 / 1536
Present study	May 2002	35	75 / 2370

Table 3
Estimates of the East Greenland Current liquid freshwater transport in the Fram Strait, given in units of mSv / km^3 y^{-1}. All studies yielded transports towards the Atlantic. S_R is the reference salinity used in the transport calculations. The estimate of Dickson et al. (2007) pertains to the transport associated with the flow of upper water. Note that the geostrophic AO-02 estimate of $M_F(34.5)$ is listed here.

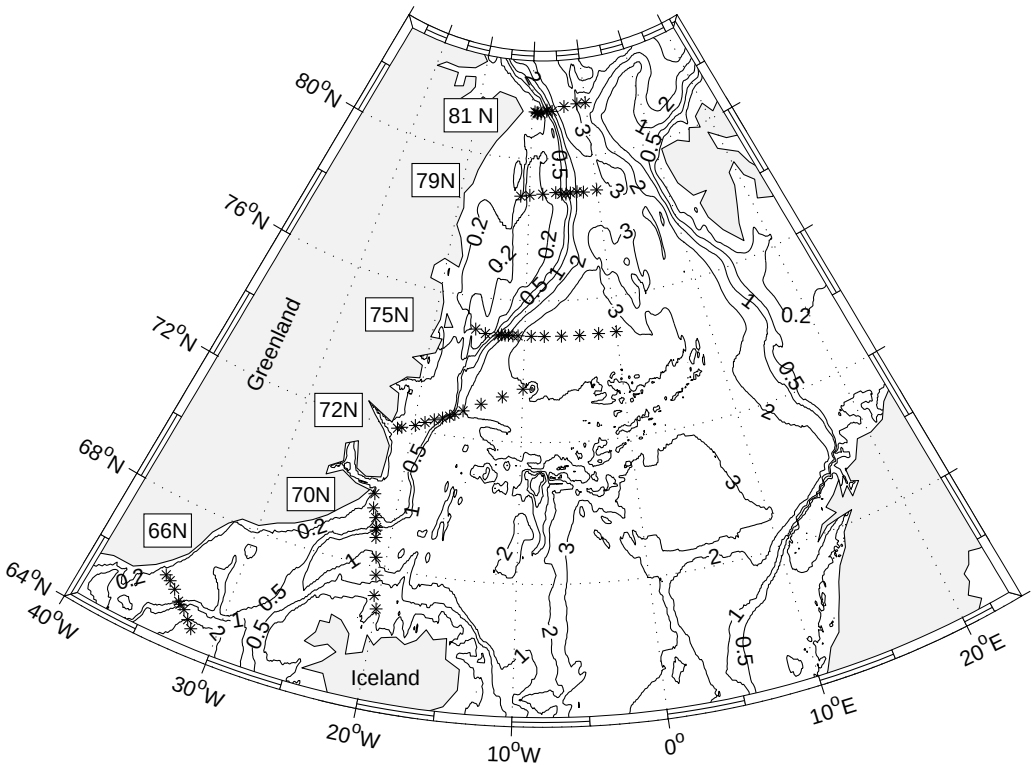

Figure 1. Map of the hydrographic stations of the AO-02 expedition that are analyzed in the present study; see Rudels et al. (2005) for a detailed description of the AO-02 hydrography measurements. The latitude labels refer to the latitude of the westernmost station of the sections. Depth contours are given in km.

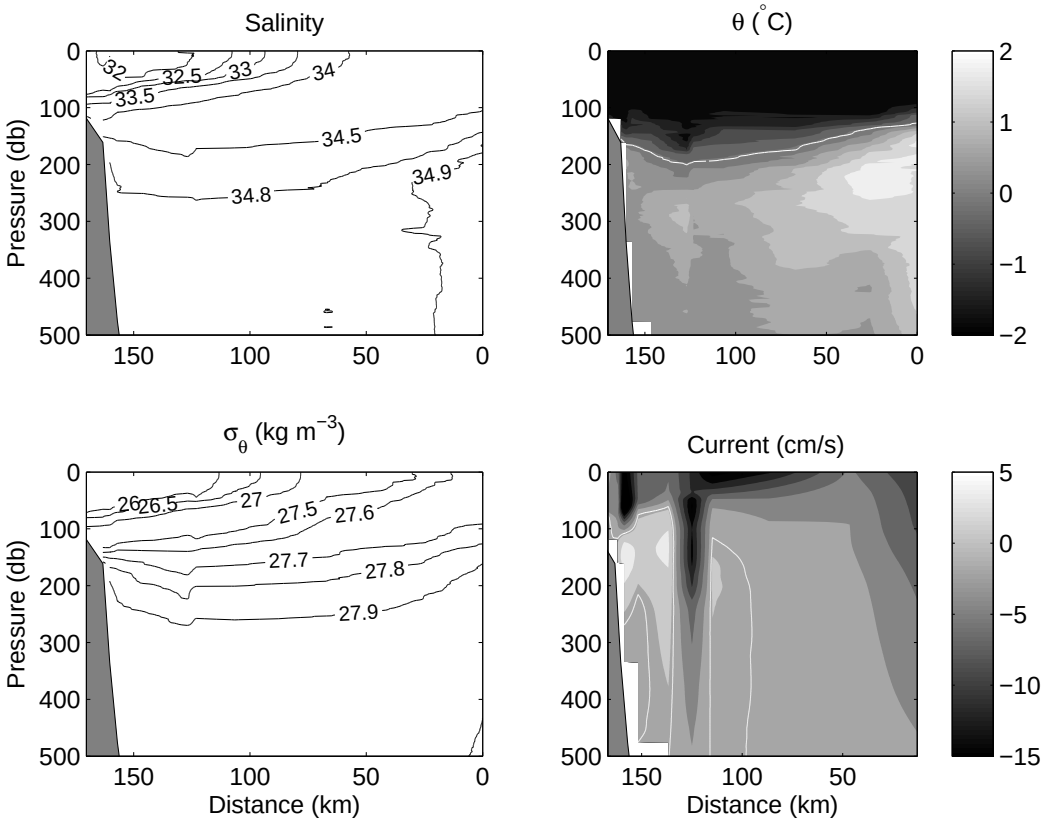

Figure 2. Hydrographic conditions and geostrophic flow in the 81°N section. The Greenland Continental Slope is located to the left. The velocity is computed using the thermal-wind relation [Eq. (7)] assuming zero flow at the bottom. Flow towards the Arctic is counted as positive. For potential temperature and velocity, the zero-isolines are marked with white lines. The entire section was ice covered.

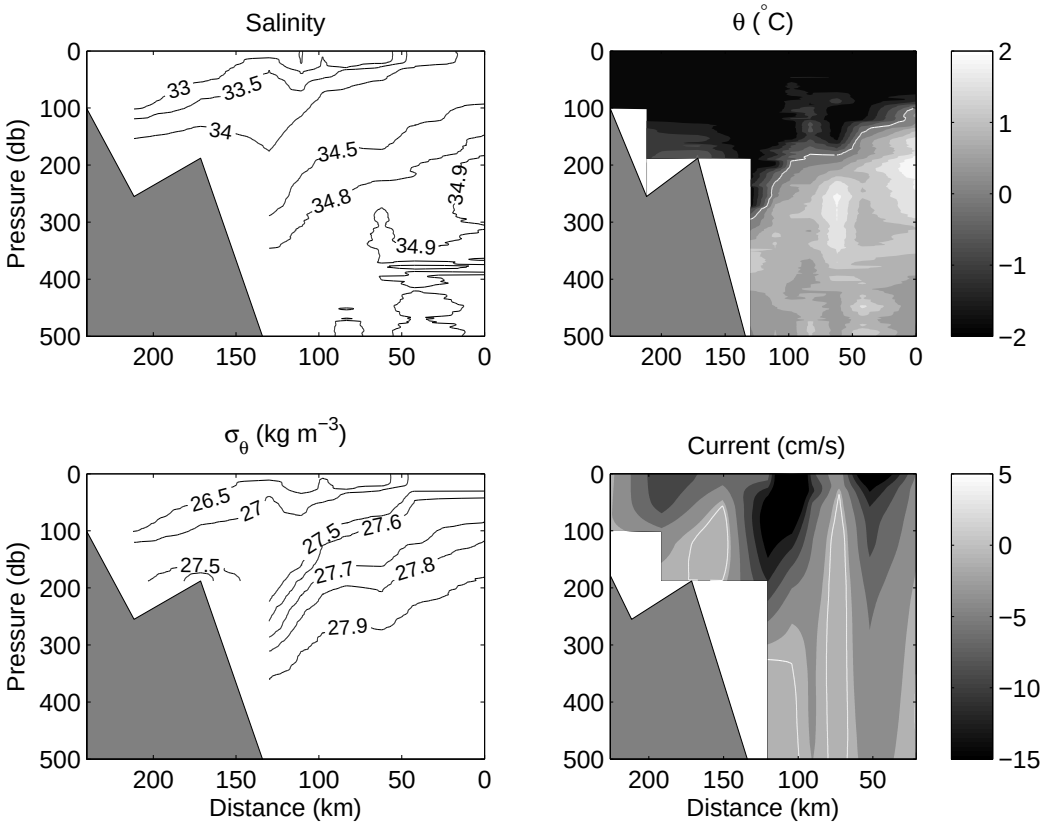

Figure 3. Hydrographic conditions and geostrophic flow in the 79°N section, located in the western part of the Fram Strait. The entire section was ice covered.

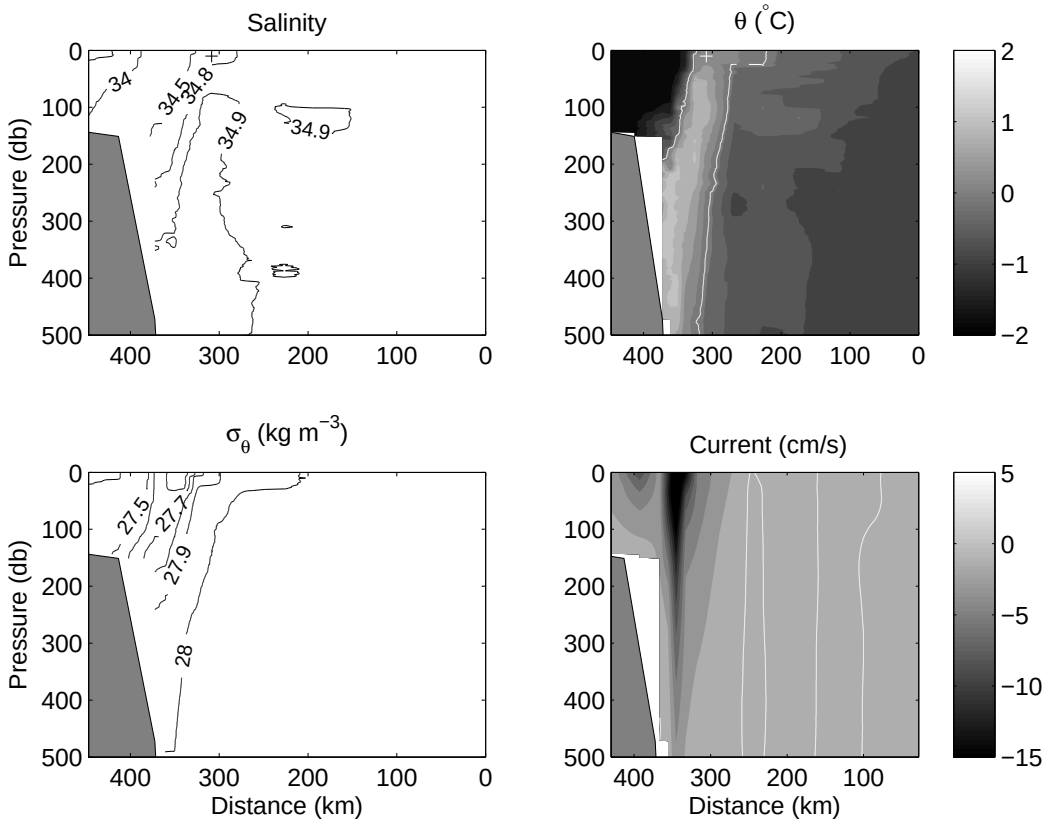

Figure 4. Hydrographic conditions and geostrophic flow in the 75°N section, traversing western part of the central Greenland Sea. Note that the core of the low-salinity ($S < 33$) PSW was not encountered in the transect. The location of the ice edge is indicated by the plus signs in the upper panels.

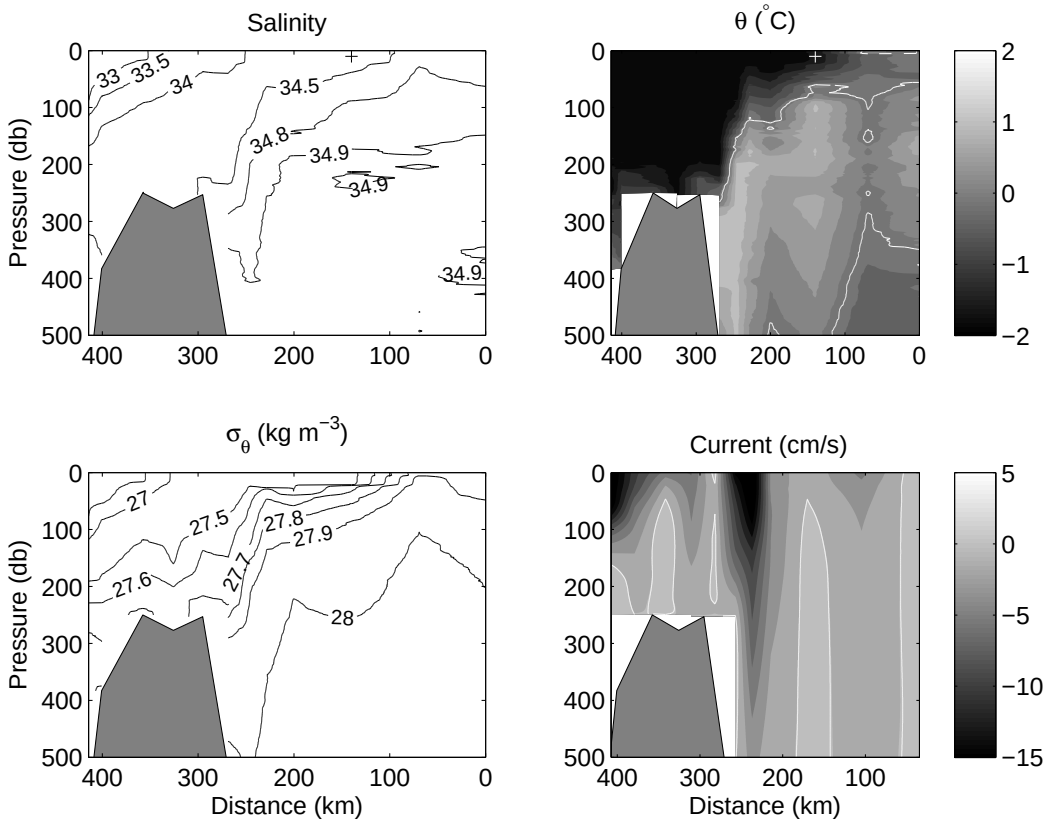

Figure 5. Hydrographic conditions and geostrophic flow in the 72°N section, traversing the southern Greenland Sea. The location of the ice edge is indicated by the plus signs in the upper panels.

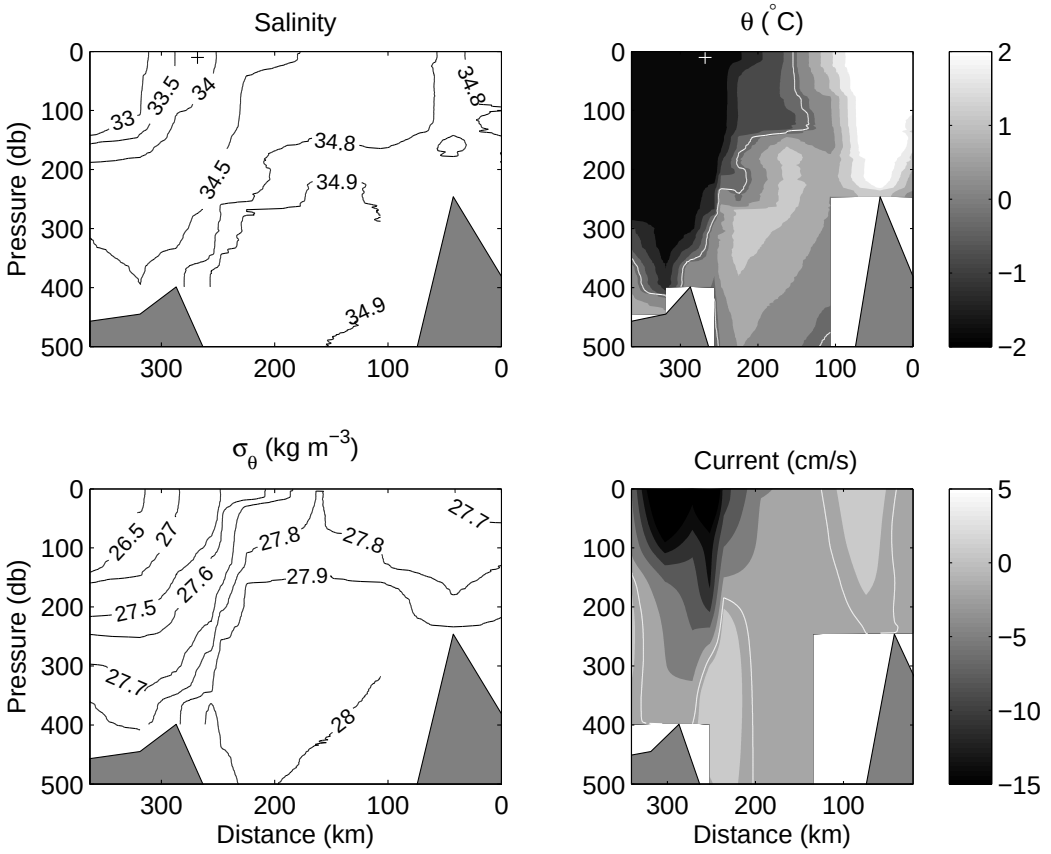

Figure 6. Hydrographic conditions and geostrophic flow in the 70°N section, traversing the Iceland Sea. The Iceland Continental Slope is visible to the right in the graphs. The location of the ice edge is indicated by the plus signs in the upper panels.

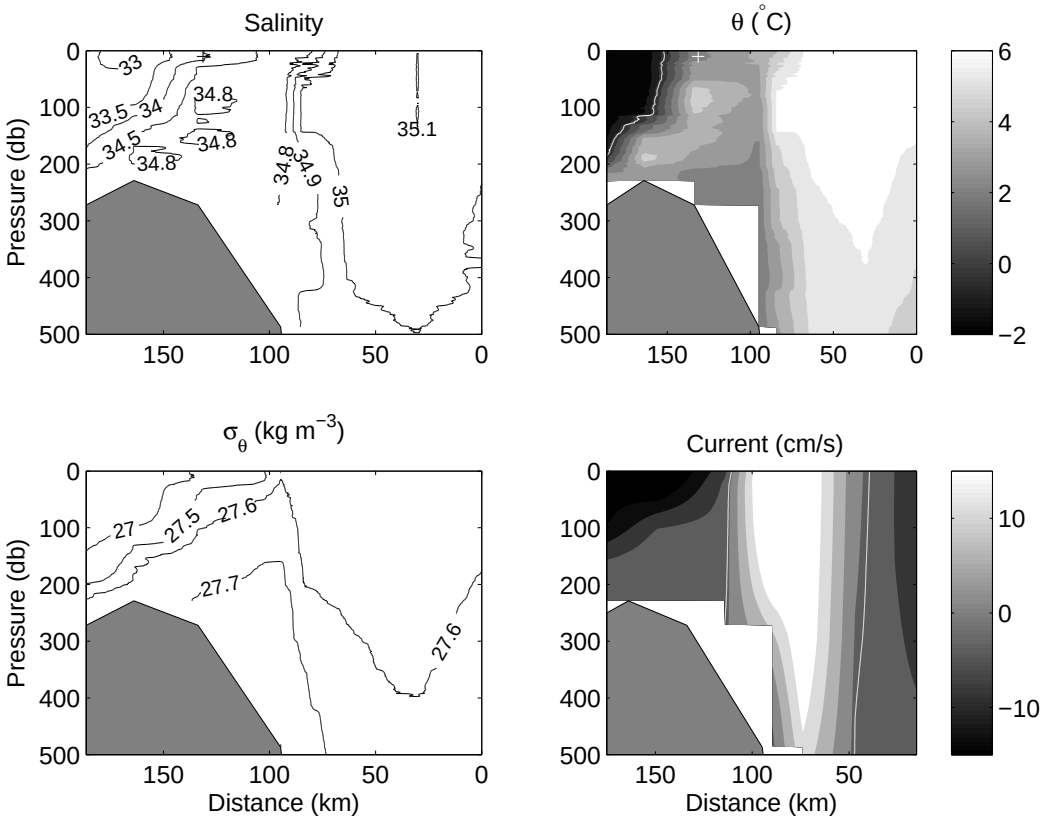

Figure 7. Hydrographic conditions at 66°N, located south of the Denmark Strait. Note the presence of Atlantic water on the seaward (right hand) side. The location of the ice edge is indicated by the plus signs in the upper panels.

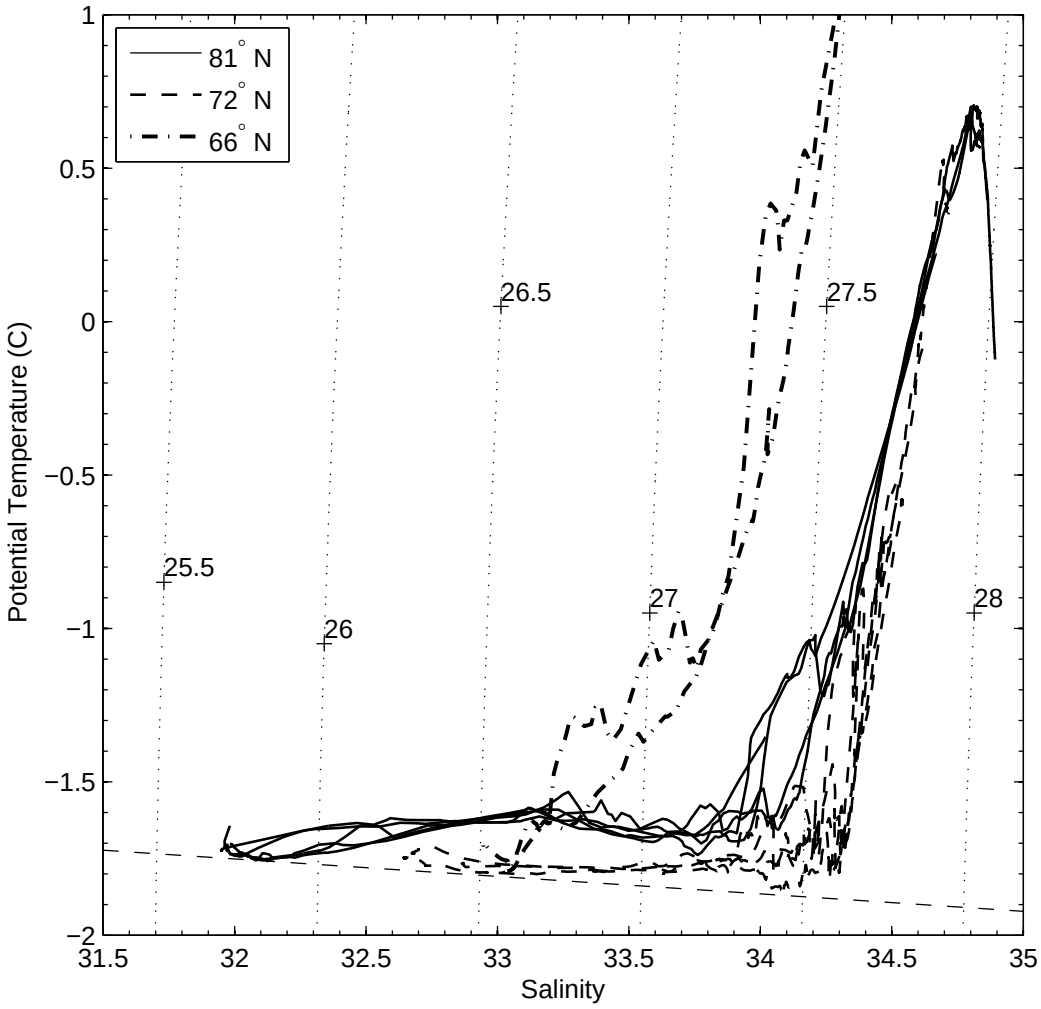

Figure 8. Potential temperature–salinity diagram of near-coastal stations at 81°N (black lines), 72 °N (dashed lines), and 66°N (dash-dotted lines). At 66°N, PSW was encountered only at two the westernmost stations. The lower dashed line shows the freezing point.

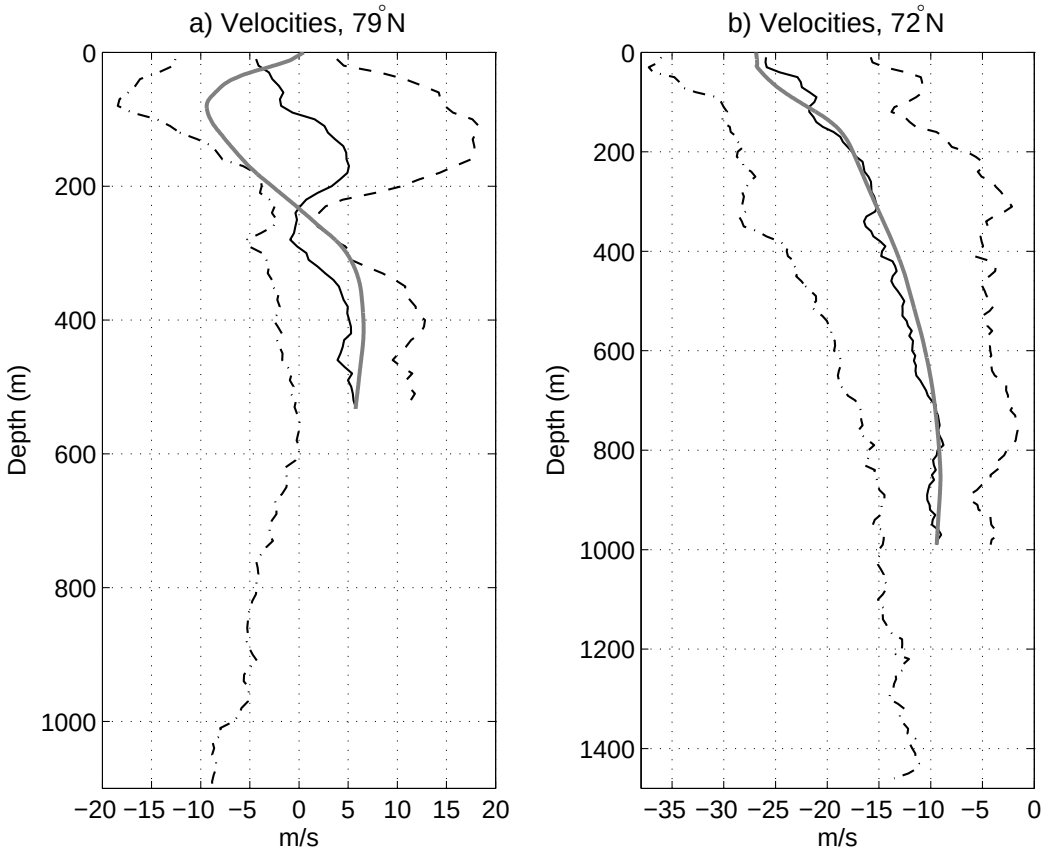

Figure 9. North (positive)-south (negative) velocities from LADCP for a) 79°N and b) 72°N (black lines). The dashed and dashed-dotted lines show the velocity profiles from two adjacent stations on the continental slope. The solid line shows the average LADCP velocity for the two stations, whereas the grey line shows the geostrophic velocity calculated from the horizontal density difference between the stations. Note that the mean bottom LADCP velocity has been added to the geostrophic flow profile.

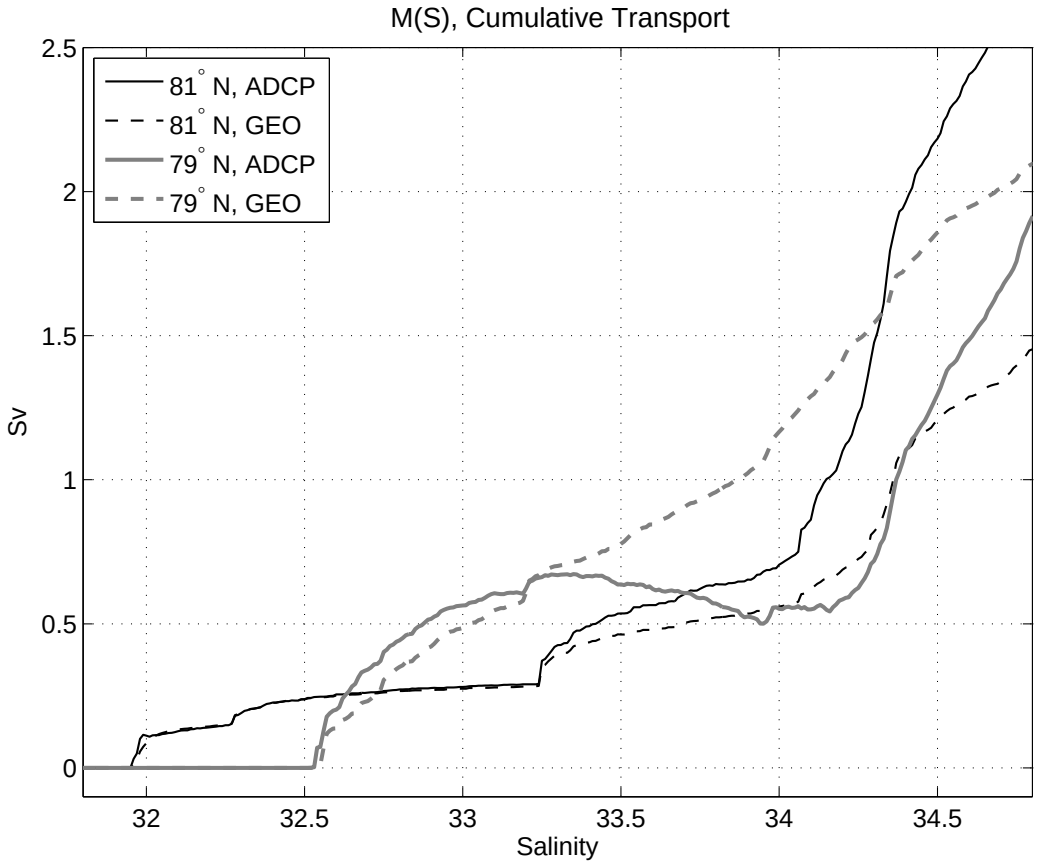

Figure 10. Cumulative transport $M(S)$, in the 81°N and 79°N sections, computed using geostrophic flow relative to zero bottom velocity (GEO) and LADCP-derived velocities (ADCP). For each section, $M(S)$ gives the net volume transport of water having a salinity less than S; see Eq. (1). Positive values of M imply transports towards the Atlantic.

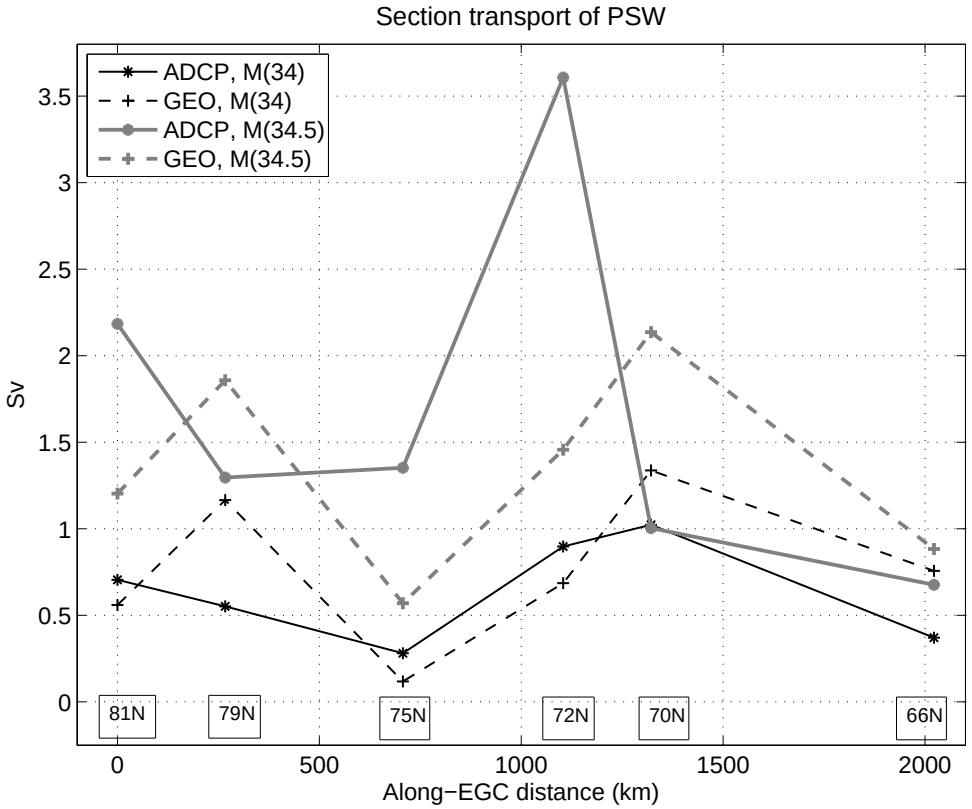

Figure 11. Along-EGC transport of Polar Surface Water measured by $M(34)$ (black lines) and $M(34.5)$ (grey lines). Results from computations with LADCP and geostrophic velocities are indicated by solid and dashed lines, respectively.

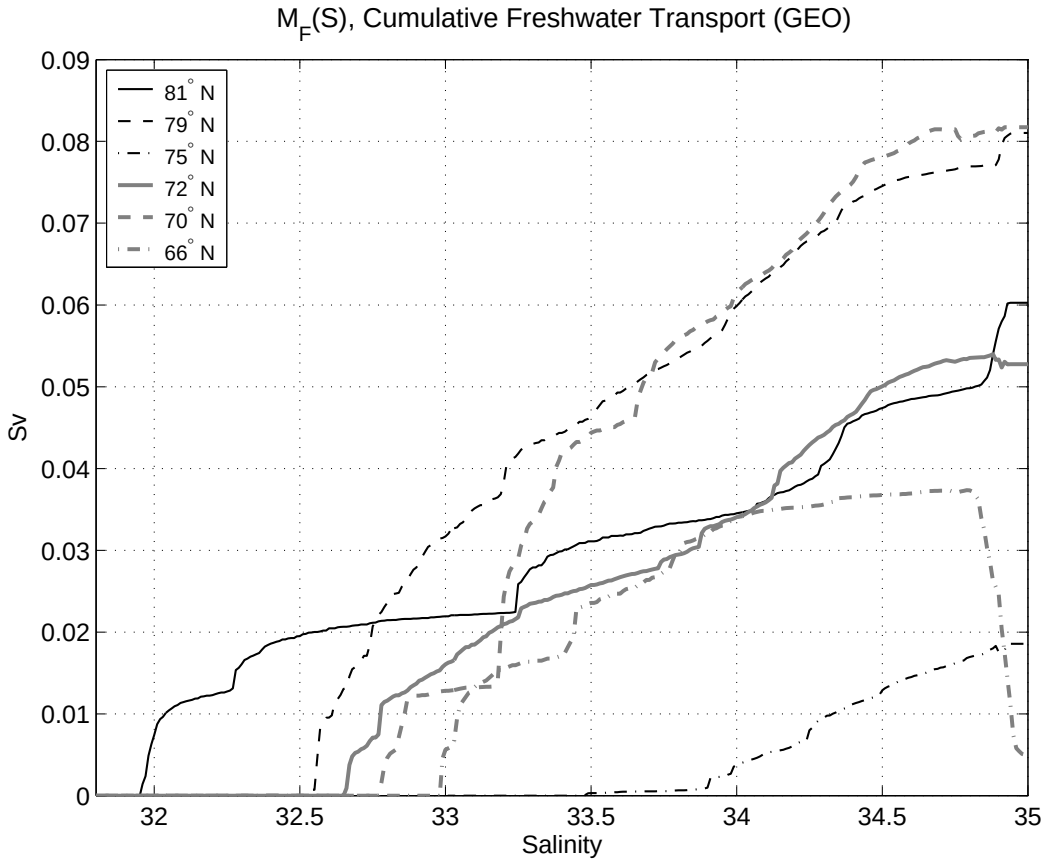

Figure 12. Cumulative freshwater transport $M_F(S)$ for the AO-02 sections. Here $M_F(S)$ is based on the geostrophic velocity estimates relative to zero bottom flow using $S_R = 35.0$; see Eq. (5). Positive values of M_F imply freshwater transports towards the Atlantic.

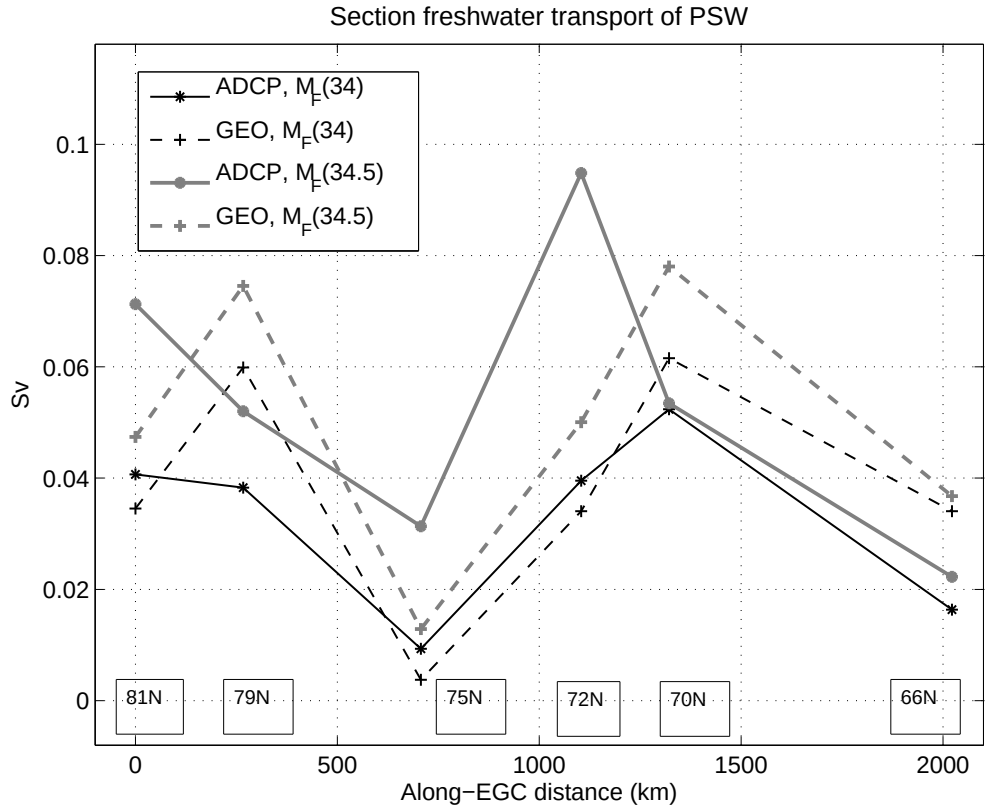

Figure 13. Along-EGC freshwater transport measured by $M_F(34)$ (black lines) and $M_F(34.5)$ (grey lines). Results from computations with LADCP and geostrophic velocities are indicated by solid and dashed lines, respectively.